2023 62nd IEEE Conference on Decision and Control (CDC)
December 13-15, 2023. Marina Bay Sands, Singapore

Estimation of regions of attraction with formal certificates in a purely data-driven setting

A. Mauroy and A. Sootla

***Abstract*— We provide a Koopman operator based method to estimate the region of attraction of equilibria in a purely data-driven setting. The proposed method yields formal stability certificates, while not requiring prior knowledge of the system dynamics or online addition of data points along the way. It consists in three steps. First, a candidate Lyapunov is constructed through an approximated linear lifted dynamics. Next, the validity domain of the Lyapunov function is assessed from the data set. This validation step is performed with the sole knowledge of a (possibly loose) second-order bound on the flow, and without the usual a priori knowledge of a Lipschitz constant. Finally, an inner approximation of the region of attraction is obtained on an adaptive grid via a branch-and-bound algorithm.**

I. Introduction

Estimating regions of attraction (ROA) of stable equilibria is an important problem in system analysis and control design, and a crucial issue in safety-critical applications. This problem has been the focus of intense research activity (see e.g. [4], [13], [14]) and, in particular, recent years have witnessed the development of ROA estimation methods in a data-driven context. However, most data-driven methods developed so far rely on adaptive sampling, that is, they use data generated *at will* by a *known* dynamical system. This is for instance the case of the work [2], which yields accurate estimations of ROA with complex geometry, but at the expense of adding data points when and where it is needed as the algorithm proceeds. Along the same lines, recent methods leveraging machine learning and neural networks in particular (see e.g. [5], [12]) require data points that are typically generated on the fly during the training process. Alternatively, [16] computes a candidate Lyapunov function from data, but utilizes the supposedly known dynamics to validate that function.

In fact, there are surprisingly few methods addressing the ROA estimation problem in a pure data-driven setting, that is, where an *unknown* dynamical system is described by a dataset given *once and for all* prior to any computation. Such a setting is considered in [6], where the authors use semi-definite programming and the so-called scenario approach to obtain common Lyapunov functions in the specific case of linear switched systems. In a similar setting, infinite-dimensional linear programming is leveraged in [7] to estimate outer approximations of (controlled) invariant sets. These two methods mostly rely on probabilistic guarantees and, to the authors' knowledge, there is no similar method which yields formal stability certificates associated with inner approximations of the ROA.

In this paper, we present a novel method for the ROA estimation problem which addresses the above-mentioned limitations. Building on our previous work [9], we rely on the Koopman operator framework, which is amenable to both stability analysis (e.g. [8]) and data-driven techniques (e.g. [15]). In particular, we construct a candidate Lyapunov function from an approximation of the Koopman operator, assess the validity of that function in a data-driven fashion, and estimate the ROA with sublevel sets of the function. Our approach is related to the recent works [5], [16] which also rely on Koopman operator theory, but it differs in the validation step, which in our case provides formal stability certificates in the purely data-driven setting described above (i.e. unknown vector field and no adaptive sampling). Moreover, while data-driven methods providing strict stability guarantees usually require the knowledge of global Lipschitz bounds of the flow map, we depart from such an assumption. Instead, we require a (possibly loose) bound on the Hessian matrix of the flow map and compute *local* Lipschitz constants from the data, a technique which also prevents us from obtaining conservative stability certificates due to large Lipschitz bounds in instability regions.

The rest of the paper is organized as follows. In Section II, we present our problem setting and introduce the Koopman operator framework with associated stability results. Our data-driven method is described in detail in Section III and illustrated with numerical examples in Section IV. Concluding remarks and perspectives are given in Section V.

II. Preliminaries

A. Problem setting

We consider a continuous-time dynamical system on a compact set $X \subset \mathbb{R}^n$ described by a flow map $\varphi : \mathbb{R}^+ \times X \to X \subset \mathbb{R}^n$. We will make the following standing assumption.

Assumption 1: The dynamical system admits an asymptotically exponentially stable equilibrium $\mathbf{x}^* \in X$.

Assumption 2: The flow map $\varphi(t, \mathbf{x})$ is continuous in t and twice continuously differentiable in $\mathbf{x}$.

With this second assumption, we can define the *Hessian bound* of the flow map.

Definition 1: A Hessian bound of the flow map φ is a function $H : \mathbb{R}^+ \to \mathbb{R}^+$ that satisfies

$$\|\nabla^2_{\mathbf{x}} \varphi_l(t, \mathbf{x})\|_2 \leq H(t)$$

A. Mauroy is with the Department of Mathematics and the Namur Research Institute for Complex Systems, University of Namur, Namur, Belgium alexandre.mauroy@unamur.be

A. Sootla is with Byju's AI Lab, London, United Kingdom aivar.sootla@gmail.com

for all $\mathbf{x} \in X$ and for all $l = 1, \ldots, n$, with the Hessian matrix $[\nabla^2_{\mathbf{x}} \varphi_l(\mathbf{x})]_{ij} = \frac{\partial^2 \varphi_l}{\partial x_i \partial x_j}(t, \mathbf{x})$.

Our data-driven stability problem is defined as follows.

Data-driven stability problem: Suppose that we are given

1) a set of K data pairs $(\mathbf{x}_k, \mathbf{y}_k = \varphi(\Delta t, \mathbf{x}_k)) \in X \times X$, where $\Delta t > 0$ is the sampling time,
2) the value of a Hessian bound $\overline{H} = H(\Delta t)$.

Then, we aim at finding the largest set X_0 and the smallest set X_1, with $X_1 \subset X_0 \subset X$, such that X_1 is *attractive* in X_0 according to the following definition.

Definition 2: A set X_1 is attractive in X_0 if, for all $\mathbf{x}_0 \in X_0$, there exists $T > 0$ such that $\varphi(T, \mathbf{x}_0) \in X_1$.

Note that we are bound to consider convergence to a set and not to a point due to the data-driven nature of the problem.

We will solve the above problem by constructing a candidate Lyapunov function V and by considering its sublevel sets

$$\begin{aligned} \Omega_\alpha &= \{\mathbf{x} \in X | V(\mathbf{x}) \leq \alpha\} \\ \Omega_{\alpha,\beta} &= \{\mathbf{x} \in X | \alpha \leq V(\mathbf{x}) \leq \beta\}. \end{aligned}$$

In particular, we will rely on the following result.

Proposition 1: Let $V : \mathbb{R}^n \to \mathbb{R}$ be a continuous function that satisfies $V(\mathbf{x}) \geq 0$ for all $\mathbf{x} \in X$, and consider the set

$$\overline{X} = \{\mathbf{x} \in X \, : \, V(\varphi(\Delta t, \mathbf{x})) < V(\mathbf{x})\}.$$

Then, for all $\alpha_1 < \alpha_0$ such that $\Omega_{\alpha_1,\alpha_0} \subset \overline{X}$, Ω_{α_1} is attractive in Ω_{α_0}. Moreover, if $\mathbf{x} \in \Omega_{\alpha_1}$ and $\varphi(t, \mathbf{x}) \notin \Omega_{\alpha_1}$ for some $t > 0$, then $\exists t_0 \in [t, t + \Delta t]$ such that $\varphi(t_0, \mathbf{x}) \in \Omega_{\alpha_1}$.

Proof: The proof follows standard arguments in stability theory and is given here for the sake of completeness. Suppose that the set Ω_{α_1} is not attractive so that, for some $\mathbf{x} \in \Omega_{\alpha_0}$, $\varphi(t, \mathbf{x}) \notin \Omega_{\alpha_1}$ for all $t \geq 0$. However, it is clear that $\varphi(t, \mathbf{x}) \in \Omega_{\alpha_0}$ (and therefore $\varphi(t, \mathbf{x}) \in \Omega_{\alpha_1,\alpha_0}$) for all $t \geq 0$ since $\Omega_{\alpha_0} \subset \overline{X}$. Moreover, the continuous function $\Delta V(\cdot) := V(\varphi(\Delta t, \cdot)) - V(\cdot)$ attains its maximal value Δ_M on the compact set $\Omega_{\alpha_1,\alpha_0}$, which satisfies $\Delta_M < 0$ since $\Omega_{\alpha_1,\alpha_0} \subset \overline{X}$. Then, we have

$$V(\varphi(N\Delta t, \mathbf{x}) = V(\mathbf{x}) + \sum_{k=0}^{N} \Delta V(\varphi(k\Delta t, \mathbf{x})) \leq V(\mathbf{x}) + N\Delta_M.$$

For $N > V(\mathbf{x})/|\Delta_M|$, it follows that $V(\varphi(N\Delta t, \mathbf{x}) < 0$, which is impossible. By contradiction, Ω_{α_1} is attractive in Ω_{α_0}.

Now suppose that $\mathbf{x} \in \Omega_{\alpha_1}$ and $\varphi(t, \mathbf{x}) \notin \Omega_{\alpha_1}$. By continuity of $V(\varphi(\cdot, \mathbf{x}))$ and the intermediate value theorem, there exist times $t_k \in [0, t]$ such that $V(\varphi(t_k, \mathbf{x})) = \alpha_1$, that is $\varphi(t_k, \mathbf{x}) \in \Omega_{\alpha_1,\alpha_0} \subset \overline{X}$. Therefore, $V(\varphi(t_k + \Delta t, \mathbf{x})) \leq \alpha_1 + \Delta_M < \alpha_1$, so that $\varphi(t_k + \Delta t, \mathbf{x}) \in \Omega_{\alpha_1}$. The result follows by setting $t_0 = \max_k t_k + \Delta t$ and noting that $t_0 \in [t, t + \Delta t]$ since $\max_k t_k \leq t$ and $t_0 > t$ (if $t_0 < t$, then there would exist a time $t' \in [t_0, t]$, i.e. $t' > \max_k t_k$, such that $V(\varphi(t', \mathbf{x})) = \alpha_1$, which is impossible). ■

B. Koopman operator framework and stability results

We briefly describe the Koopman operator framework that we leverage in the context of data-driven stability analysis. The Koopman operator associated with the discrete-time map $\mathbf{x} \mapsto \varphi(\Delta t, \mathbf{x})$ is the linear operator $U : C(X) \to C(X)$ defined by $(Uf)(\mathbf{x}) = f \circ \varphi(\Delta t, \mathbf{x})$ for all *observables* $f \in C(X)$.

For a chosen subspace $\mathcal{F}_N \subset C(X)$, the Koopman operator U can be approximated by its compression $U_N = P_N U|_{\mathcal{F}_N}$, where $P_N : C(X) \to \mathcal{F}_N$ is a projection operator. The compression operator U_N is finite-dimensional and can therefore be represented by a matrix $\mathbf{U}$. Note that, when data are available, the matrix representation $\mathbf{U}$ can be obtained through the extended dynamic mode decomposition (EDMD) method [15] (see Section III-A). Moreover, for a set of N basis functions $\{\psi_j\}_{j=1}^N$ such that $\mathcal{F}_N = \text{span}\{\psi_j\}_{j=1}^N$, the dynamics of the lifted state $\mathbf{\Psi}(\mathbf{x}) = (\psi_1(\mathbf{x}) \ \ldots \ \psi_N(\mathbf{x}))^T$ can be approximated by (see e.g. [10, Chapter 1])

$$\mathbf{\Psi}(\varphi(\Delta t, \mathbf{x})) = \mathbf{U}^T \mathbf{\Psi}(\mathbf{x}) + \varepsilon(\mathbf{x}), \tag{1}$$

where $\varepsilon(\mathbf{x})$ is the approximation error. As shown in [9], this can be used to derive a candidate Lyapunov function V for the system. Indeed, provided that the matrix $\mathbf{U}$ is stable (i.e. its eigenvalues lie inside the unit circle) and that $\mathbf{\Psi}(\mathbf{x})$ is injective at $\mathbf{x}^*$, there exists a matrix $\mathbf{Q} \succ \mathbf{0}$ such that $V(\mathbf{x}) = \mathbf{\Psi}^{\mathrm{T}}(\mathbf{x}) \mathbf{Q} \mathbf{\Psi}(\mathbf{x})$ is a candidate Lyapunov function. More precisely, we have the following result, where the $\mathcal{H}_\infty$ norm of a (discrete-time) transfer function $\mathbf{G}$ is defined by

$$\|\mathbf{G}(z)\|_{\mathcal{H}_\infty} = \sup_{\omega \in \mathbb{R}} s(\mathbf{G}(e^{i\omega}))$$

with $s(\mathbf{G}(e^{i\omega}))$ the largest singular value of the matrix $\mathbf{G}(e^{i\omega})$.

Theorem 1: Let $\mathbf{U}$ be the matrix representation of the Koopman operator U in the subspace spanned over $\{\psi_j\}_{j=1}^N$ with $\mathbf{\Psi}(\mathbf{x}) = \mathbf{0}$ if and only if $\mathbf{x} = \mathbf{x}^*$. If there exist positive semidefinite matrices $\mathbf{Z}$, $\mathbf{W}$ such that

$$\|\mathbf{W}^{1/2}(zI - \mathbf{U}^T)^{-1}\mathbf{Z}^{-1/2}\|_{\mathcal{H}_\infty} < 1 \tag{2}$$

and

$$\sup_{\mathbf{x} \in X} \frac{\|\mathbf{Z}^{1/2} \varepsilon(\mathbf{x})\|_2}{\|\mathbf{W}^{1/2} \mathbf{\Psi}(\mathbf{x})\|_2} < 1 \quad \forall \mathbf{x} \in \overline{X}', \tag{3}$$

then the system admits on $\overline{X}' \subseteq \overline{X}$ a Lyapunov function of the form $V(\mathbf{x}) = \mathbf{\Psi}^{\mathrm{T}}(\mathbf{x}) \mathbf{Q} \mathbf{\Psi}(\mathbf{x})$, with $\mathbf{Q} \succ \mathbf{0}$, i.e. $V(\varphi(\Delta t, \mathbf{x})) < V(\mathbf{x})$ for all $\mathbf{x} \in \overline{X}' \setminus \{\mathbf{x}^*\}$.

Proof: The function $V(\mathbf{x})$ is positive on X for all $\mathbf{x} \neq \mathbf{x}^*$. Moreover, we have

$$\Delta V(\mathbf{x}) = \mathbf{\Psi}^{\mathrm{T}}(\varphi(\Delta t, \mathbf{x})) \mathbf{Q} \mathbf{\Psi}(\varphi(\Delta t, \mathbf{x})) - \mathbf{\Psi}^{\mathrm{T}}(\mathbf{x}) \mathbf{Q} \mathbf{\Psi}(\mathbf{x}).$$

Denoting $\mathbf{y} = \mathbf{\Psi}(\mathbf{x})$, $\mathbf{w} = \varepsilon(\mathbf{x})$ and using (1), we obtain

$$\begin{aligned} \Delta V(\mathbf{x}) &= (\mathbf{U}^{\mathrm{T}}\mathbf{y} + \mathbf{w})^{\mathrm{T}} \mathbf{Q} (\mathbf{U}^{\mathrm{T}}\mathbf{y} + \mathbf{w}) - \mathbf{y}^{\mathrm{T}} \mathbf{Q} \mathbf{y} \\ &= \mathbf{y}^{\mathrm{T}}(\mathbf{U}\mathbf{Q}^{\mathrm{T}}\mathbf{U} - \mathbf{Q})\mathbf{y} + 2\mathbf{y}^{\mathrm{T}}(\mathbf{U}\mathbf{Q})\mathbf{w} + \mathbf{w}^{\mathrm{T}}\mathbf{Q}\mathbf{w}. \end{aligned}$$

Next, we can use the inequality

$$2\mathbf{y}^{\mathrm{T}}(\mathbf{U}\mathbf{Q})\mathbf{w} \leq \mathbf{y}^{\mathrm{T}}\mathbf{U}\mathbf{Q}\tilde{\mathbf{Z}}^{-1}\mathbf{Q}\mathbf{U}^{\mathrm{T}}\mathbf{y} + \mathbf{w}^{\mathrm{T}}\tilde{\mathbf{Z}}\mathbf{w}$$

which is valid for any $\tilde{\mathbf{Z}} \succ \mathbf{0}$. For $\tilde{\mathbf{Z}} = \mathbf{Z} - \mathbf{Q}$ with $\mathbf{Z} \succ \mathbf{Q}$, we get

$$\Delta V(\mathbf{x}) \leq \mathbf{y}^{\mathrm{T}}(\mathbf{U}\mathbf{Q}\mathbf{U}^{\mathrm{T}} - \mathbf{Q} + \mathbf{U}\mathbf{Q}(\mathbf{Z}-\mathbf{Q})^{-1}\mathbf{Q}\mathbf{U}^{\mathrm{T}} + \mathbf{W})\mathbf{y} + \mathbf{w}^{\mathrm{T}}\mathbf{Z}\mathbf{w} - \mathbf{y}^{\mathrm{T}}\mathbf{W}\mathbf{y}.$$

Now, if $\mathbf{Z}$ and $\mathbf{W}$ are such that $\|\mathbf{W}^{1/2}(\mathbf{I}z - \mathbf{U}^{\mathrm{T}})^{-1}\mathbf{Z}^{-1/2}\|_{\mathcal{H}_\infty} < 1$, then there exists $\mathbf{Q}$ such that (see e.g. [17, Corollary 21.17])

$$\mathbf{U}\mathbf{Q}\mathbf{Z}^{-1/2}(\mathbf{I} - \mathbf{Z}^{-1/2}\mathbf{Q}\mathbf{Z}^{-1/2})^{-1}\mathbf{Z}^{-1/2}\mathbf{Q}\mathbf{U}^{\mathrm{T}} + \mathbf{W} \prec \mathbf{0}$$

or equivalently

$$\mathbf{U}\mathbf{Q}\mathbf{U}^{\mathrm{T}} - \mathbf{Q} + \mathbf{U}\mathbf{Q}(\mathbf{Z}-\mathbf{Q})^{-1}\mathbf{Q}\mathbf{U}^{\mathrm{T}} + \mathbf{W} \prec \mathbf{0}. \quad (4)$$

Under the above condition, we then obtain $\Delta V(\mathbf{x}) < 0$ if $\varepsilon^{\mathrm{T}}(\mathbf{x})\mathbf{Z}\varepsilon(\mathbf{x})) \leq \mathbf{\Psi}^{\mathrm{T}}(\mathbf{x})\mathbf{W}\mathbf{\Psi}(\mathbf{x})$. ∎

This result can be recognized as a variation of the small-gain theorem, and is a generalization of the result in [9], where a continuous-time and non-weighted small gain result (i.e., $\mathbf{W} = \mathbf{Z} = \mathbf{I}$) was considered.

A typical problem is to choose the weights $\mathbf{W}$ and $\mathbf{Z}$ so that the $\mathcal{H}_\infty$ norm of the system is smaller than one. This choice can be guided by the construction proposed in [8] (and used in [5], [16]), where a Lyapunov function is built with the eigenfunctions of the Koopman operator. These eigenfunctions can be approximated by the eigenvectors of $\mathbf{U}$ (see e.g. [10, Chapter 1]). Therefore, we can consider the Lyapunov function $\mathbf{\Psi}^{\mathrm{T}}(\mathbf{x})\mathbf{S}^*\mathbf{\Sigma}\mathbf{S}\mathbf{\Psi}(\mathbf{x})$ for some positive definite $\mathbf{\Sigma}$, where the matrix $\mathbf{S}$ is a collection eigenvectors of $\mathbf{U}$ such that $\mathbf{S}\mathbf{U}^{\mathrm{T}} = \mathbf{\Lambda}\mathbf{S}$ with $\mathbf{\Lambda} = \mathrm{diag}(\lambda_1, \ldots, \lambda_N)$ the diagonal matrix containing the associated eigenvalues. In this case, we have to set $\mathbf{Q} = \mathbf{S}^*\mathbf{\Sigma}\mathbf{S}$, which is a real-valued positive definite matrix as long as $\mathbf{U}$ is diagonalizable. Also, it can be shown that the weight matrices $\mathbf{W}$ and $\mathbf{Z}$ satisfying the $\mathcal{H}_\infty$ norm constraint and such that $\mathbf{Q} = \mathbf{S}^*\mathbf{\Sigma}\mathbf{S}$ can be chosen according to

$$\mathbf{W} = \delta\, \mathbf{S}^*\mathbf{\Sigma}\mathbf{S} \qquad \mathbf{Z} = \delta^{-1}\mathbf{S}^*\mathbf{\Sigma}\mathbf{S} \quad (5)$$

with $\delta \in (0, 1 - \max_i |\lambda_i|)$. See Appendix A for detailed developments.

III. Data-driven method for ROA estimation

We are now in a position to describe our data-driven method for ROA estimation. We will consider the following steps. Using the data and relying on Theorem 1, we construct a candidate Lyapunov function through the Koopman operator framework. Then, instead of estimating the possibly conservative region $\overline{X}'$ where condition (3) is satisfied, we directly estimate the validity region $\overline{X}$ on which the Lyapunov function is decreasing. Finally, we find the largest value α_0 and the smallest value α_1 that satisfy the assumptions of Proposition 1, so that that $X_1 = \Omega_{\alpha_1}$ is attractive in $X_0 = \Omega_{\alpha_0}$, which stands for an inner approximation of the ROA.

A. Construction of the Lyapunov function

We first use the EDMD method (see [15]) to obtain the matrix approximation

$$\mathbf{U} = \mathbf{\Psi}_{\mathbf{X}}^{\dagger}\mathbf{\Psi}_{\mathbf{Y}} \quad (6)$$

where $\dagger$ denotes the Moore-Penrose pseudoinverse and with the $N \times K$ data matrices

$$\mathbf{\Psi}_{\mathbf{X}} = \begin{pmatrix} \psi_1(\mathbf{x}_1) & \cdots & \psi_1(\mathbf{x}_K) \\ \vdots & \ddots & \vdots \\ \psi_N(\mathbf{x}_1) & \cdots & \psi_N(\mathbf{x}_K) \end{pmatrix}$$

$$\mathbf{\Psi}_{\mathbf{Y}} = \begin{pmatrix} \psi_1(\mathbf{y}_1) & \cdots & \psi_1(\mathbf{y}_K) \\ \vdots & \ddots & \vdots \\ \psi_N(\mathbf{y}_1) & \cdots & \psi_N(\mathbf{y}_K) \end{pmatrix}.$$

We will consider monomial basis functions of the form $(x_1 - x_1^*)^{\alpha_1} \cdots (x_n - x_n^*)^{\alpha_n}$, with $\alpha_1 + \cdots + \alpha_n < d_{max}$. Note that the number of basis functions should satisfy $N < K$.

Next, using Theorem 1, we compute a candidate Lyapunov function $V(\mathbf{x}) = \mathbf{\Psi}^{\mathrm{T}}(\mathbf{x})\mathbf{Q}\mathbf{\Psi}(\mathbf{x})$, through the Riccati equation (4) with $\mathbf{Z}$, $\mathbf{W}$ given by (5), and with $\mathbf{\Sigma} = \mathbf{I}$ (by default). It is noticeable that the Koopman matrix $\mathbf{U}$ can possibly be unstable (i.e. its spectral radius is larger than 1), in which case one cannot solve (4) and obtain the Lyapunov function. This can arise when many data points lie outside the basin of attraction of the equilibrium $\mathbf{x}^*$. To overcome this issue, only data points $(\mathbf{x_k}, \mathbf{y_k})$ such that $\|\mathbf{x_k} - \mathbf{x}^*\| < D_{max}$ should be used with the EDMD method to construct the data matrices $\mathbf{\Psi}_{\mathbf{X}}$ and $\mathbf{\Psi}_{\mathbf{Y}}$. The parameter D_{max} is initially set to a large value, which is gradually decreased until the Koopman matrix becomes stable.

B. Validation of the Lyapunov function

In this section, we develop our method to estimate the validity region of the Lyapunov function. To do so, we first need to estimate the local Lipschitz constants of the flow map.

1) Computation of local Lipschitz constants: We aim at computing a function $L_l : X \to \mathbb{R}^+$, $l = 1, \ldots, n$, such that

$$\|\nabla_{\mathbf{x}}\varphi_l(\Delta t, \mathbf{x})\| \leq L_l(\mathbf{x}).$$

Consider two pairs of data-points $(\mathbf{x}_i, \mathbf{y}_i)$ and $(\mathbf{x}_j, \mathbf{y}_j)$ with $i, j \in \{1, \ldots, K\}$ and the associated unit vector $\mathbf{e}_{ij} = (\mathbf{x}_j - \mathbf{x}_i)/\|\mathbf{x}_j - \mathbf{x}_i\|$. It follows from the mean value theorem that

$$\nabla_{\mathbf{x}}\varphi_l(\Delta t, \tilde{\mathbf{x}}) \cdot \mathbf{e}_{ij} = \frac{\mathbf{y}_j - \mathbf{y}_i}{\|\mathbf{x}_j - \mathbf{x}_i\|}$$

for some $\tilde{\mathbf{x}} = \mathbf{x}_i + \gamma(\mathbf{x}_j - \mathbf{x}_i)$ with $\gamma \in [0, 1]$. Then, for some $\bar{\mathbf{x}} = \mathbf{x} + \mu(\mathbf{x} - \tilde{\mathbf{x}})$ with $\mu \in [0, 1]$, we obtain by another application of the mean value theorem that

$$\begin{aligned} \nabla_{\mathbf{x}}\varphi_l(\Delta t, \mathbf{x}) \cdot \mathbf{e}_{ij} &= \frac{\mathbf{y}_j - \mathbf{y}_i}{\|\mathbf{x}_j - \mathbf{x}_i\|} + (\tilde{\mathbf{x}} - \mathbf{x})\nabla^2_{\mathbf{x}}\varphi_l(\Delta t, \bar{\mathbf{x}})\mathbf{e}_{ij} \\ &\leq \frac{\mathbf{y}_j - \mathbf{y}_i}{\|\mathbf{x}_j - \mathbf{x}_i\|} + \overline{H}\,\|\mathbf{x}_j - \mathbf{x}\| \triangleq C_{ij}, \end{aligned}$$

with the Hessian bound $\overline{H} = H(\Delta t)$ (see Definition 2) and where we have assumed without loss of generality that $\|\mathbf{x}_j - \mathbf{x}\| > \|\mathbf{x}_i - \mathbf{x}\|$. Next, we can rewrite $\nabla_{\mathbf{x}}\varphi_l(\Delta t, \mathbf{x}) = \|\nabla_{\mathbf{x}}\varphi_l(\Delta t, \mathbf{x})\|\,\mathbf{e}$ for some $\mathbf{e}$ such that $\|\mathbf{e}\| = 1$. By considering a set I of pairs (i, j) chosen such that the data points $\mathbf{x}_i$ and $\mathbf{x}_j$ are among the nearest neighbors of $\mathbf{x}$, we write

$$\|\nabla_{\mathbf{x}}\varphi_l(\Delta t, \mathbf{x})\| \leq \min_{(i,j)\in I} \frac{C_{ij}}{\mathbf{e}\cdot\mathbf{e}_{ij}}.$$

Since $\mathbf{e}$ is unknown, we finally obtain the Lipschitz bound by maximizing over $\mathbf{e}$:

$$\|\nabla_{\mathbf{x}}\varphi_l(\Delta t, \mathbf{x})\| \leq \max_{\|\mathbf{e}\|=1} \min_{(i,j)\in I} \frac{C_{ij}}{\mathbf{e}\cdot\mathbf{e}_{ij}} \triangleq L_l(\mathbf{x}).$$

2) Estimating the validity region: We approximate the validity region of the Lyapunov function with the set

$$\overline{X}_{balls} = \bigcup_{k=1}^{K} \mathcal{B}(\mathbf{x}_k, r_k) \cap X \subseteq \overline{X} \tag{7}$$

where $\mathcal{B}(\mathbf{x}_k, r_k)$ is a ball of radius r_k and centered at the sample point $\mathbf{x}_k$. We can note that

$$\begin{aligned}
|\varphi_l(\Delta t, \mathbf{x}) - \varphi_l(\Delta t, \mathbf{x}_k)| &= |\varphi_l(\Delta t, \mathbf{x}_k) - \mathbf{y}_k| \\
&\leq r_k \max_{\mathbf{x}\in\mathcal{B}(\mathbf{x}_k,r)} \|\nabla_{\mathbf{x}}\varphi_l(\Delta t, \mathbf{x})\| \\
&\leq r_k \left(L_l(\mathbf{x}_k) + r_k \max_{\mathbf{x}\in\mathcal{B}(\mathbf{x}_k,r)} \|\nabla_{\mathbf{x}} \left(\|\nabla_{\mathbf{x}}\varphi_l(\Delta t, \mathbf{x})\|_2\right)\|_2 \right) \\
&\leq r_k\, L_l(\mathbf{x}_k) + r_k^2\, \overline{H}
\end{aligned}$$

where we used the fact that $\|\nabla(\|\nabla f\|_2)\|_2 < \|\nabla^2 f\|_2$. Therefore,

$$\mathbf{x} \in \mathcal{B}(\mathbf{x}_k, r_k) \Rightarrow \varphi(\Delta t, \mathbf{x}) \in \mathcal{R}(\mathbf{y}_k, r_k) \tag{8}$$

with the hyperrectangle

$$\mathcal{R}(\mathbf{y}_k, r_k) \triangleq \{\mathbf{x} \in X : |x^{(l)} - y_k^{(l)}| \leq r_k\, L_l(\mathbf{x}_k) + \overline{H}\, r_k^2 \ \ \forall l\},$$

where $x^{(l)}$ denotes the lth component of $\mathbf{x}$. It follows from (8) that the largest radius r_k of a ball $\mathcal{B}(\mathbf{x}_k, r_k)$ satisfying (7), i.e. $\mathcal{B}(\mathbf{x}_k, r_k) \subset \overline{X}$, is the solution r^* to the following optimization problem:

$$\max\, r \quad \text{s.t.} \max_{\mathbf{y}\in\mathcal{R}(\mathbf{y}_k,r)} V(\mathbf{y})) \leq \min_{\mathbf{x}\in\mathcal{B}(\mathbf{x}_k,r)} V(\mathbf{x})\,. \tag{9}$$

If one can compute bounds $V_{min}(r)$ and $V_{max}(r)$ such that $\max_{\mathbf{y}\in\mathcal{R}(\mathbf{y}_k,r)} \leq V_{max}(r)$ and $\min_{\mathbf{x}\in\mathcal{B}(\mathbf{x}_k,r)} V(\mathbf{x}) \geq V_{min}(r)$, the above problem can be relaxed to

$$\max\, r \quad \text{s.t. } V_{max}(r) \leq V_{min}(r)\,.$$

Since the functions $V_{min}(r)$ and $V_{max}(r)$ are monotone decreasing and increasing, respectively, the solution r^* satisfies $V_{max}(r^*) = V_{min}(r^*)$ and can be computed by using a bisection method.

In the case of monomial basis functions, lower and upper bounds $V_{min}(r)$ and $V_{max}(r)$ could be computed using polynomial optimization (i.e. SOS programming). However, this is computationally expensive since these bounds are computed for a possibly large number K of balls. Instead, we use the methods detailed in Appendix B.

C. Finding the largest region of attraction

Now it remains to find the largest value α_0 and the smallest value α_1 such that the sublevel set $\Omega_{\alpha_1,\alpha_0}$ is contained in $\overline{X}_{balls}$ (see (7)). This amounts to solving the following problem:

$$\begin{aligned}
&\max_{\alpha_0,\alpha_1} (\alpha_0 - \alpha_1) \\
&\text{s.t.} \quad \forall \mathbf{x} \in X \setminus \bar{X}_{balls}, \quad \alpha_0 < V(\mathbf{x}) \quad \text{or} \quad \alpha_1 > V(\mathbf{x}) \\
&\qquad 0 \leq \alpha_1 \leq \alpha_0 < \min_{\mathbf{x}\in\partial X} V(\mathbf{x})\,,
\end{aligned} \tag{10}$$

where the constraint $\alpha_0 < \min_{\mathbf{x}\in\partial X} V(\mathbf{x})$ ensures that $\Omega_{\alpha_0} \subset X$. This problem is solved via a bisection algorithm. The first constraint is equivalent to the ball covering condition $\Omega_{\alpha_1,\alpha_0} \subset \bar{X}_{balls}$ and is verified with a branch-and-bound method inspired by [1]. This is done by building an adaptive grid and by checking whether every cell of the grid either has an empty intersection with $\Omega_{\alpha_1,\alpha_0}$ or is contained within a single ball $\mathcal{B}(\mathbf{x}_k, r)$ for some k. When a cell does not satisfy this condition, it is divided into smaller cells until they either satisfy the above condition or reach a preset minimal grid size. In the latter case, one concludes that the region $\Omega_{\alpha_1,\alpha_0}$ is not covered by the validity region $\bar{X}_{balls}$ and a smaller sublevel set $\Omega_{\alpha_1,\alpha_0}$ (with smaller α_0 or larger α_1) is considered at the next iteration of the bisection algorithm.

Remark 1 (Adaptive sampling): The branch-and-bound method described above is amenable to addition of data points on the fly (although this is not permitted in our original problem setting). When a cell of minimal size does not satisfy the disk covering condition, one could possibly add a new data point at the center of that cell and compute the radius of the associated ball. If the added ball covers the cell, then the algorithm can proceed.

IV. Numerical experiments

In this section, we illustrate our data-driven method with two numerical examples.

A. Two-dimensional system

We consider a damped pendulum described by

$$\begin{aligned}
\dot{x}_1 &= x_2 \\
\dot{x}_2 &= -\sin(x_1) - x_2
\end{aligned}$$

which admits a stable equilibrium at the origin and two saddle nodes at $(\pm\pi, 0)$. We consider to test cases: (i) 10000 data points are uniformly randomly distributed over $[-4, 4]^2$, (ii) data points are distributed over a uniform 100×100 grid in $[-4, 4]^2$. All data points are generated with a sampling time $\Delta t = 3$. The Hessian bound is equal to $\overline{H} = 7.12$ (estimated numerically). The basis functions are monomials of total degree up to 3 and the Koopman matrix is constructed with $D_{max} = 2$. The approximation validity region X_{balls} of the Lyapunov function is shown in Fig. 1(a) in the case of randomly distributed points. The approximation $\Omega_{\alpha_1,\alpha_0}$ of the ROA, shown in Fig. 1(b), is larger with data points distributed over a uniform grid (solid curves) than with

randomly distributed points (dashed curves). It can also be seen in Fig. 1(a) that the intersection of the balls (disks) can be large so that fewer data points would be sufficient. Numerical simulations (not shown here) demonstrate that one could indeed obtain similar results with fewer data points if adaptive sampling were permitted (see Remark 1). They also suggest that better results are obtained with our choice of matrices $\mathbf{Z}$ and $\mathbf{W}$, compared with a generic choice $\mathbf{Z} = \mathbf{W} = \mathbf{I}$.

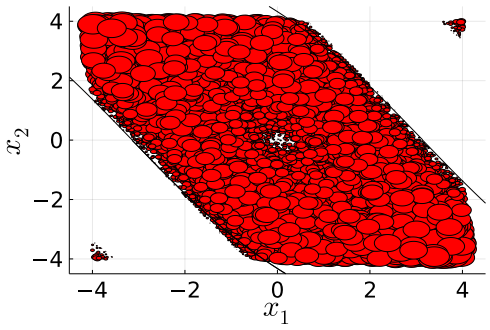

(a) Validity region of the Lyapunov function

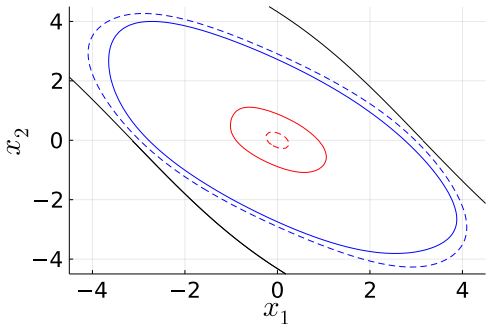

(b) Approximation of the ROA

Fig. 1. Estimation of the ROA of the origin for the pendulum dynamics. (a) The union of the red disks provide an inner approximation X_{balls} of the validity region $\overline{X}$ for the Lyapunov function (shown here in the case of randomly distributed data points). (b) The method shows that Ω_{α_1} (red curves) is attractive in the inner approximation Ω_{α_0} (blue curves) of the ROA (black curve). Solid curves: randomly distributed data points; dashed curves: data points over a uniform grid.

Remark 2: The effect of an overestimated Hessian bound on the performance is very moderate. In the above example, if we use a loose bound 50% higher than the true value (i.e. $\overline{H} = 10.68$ instead of $\overline{H} = 7.12$), the area of the estimated ROA decreases by only 2.2%. This can be explained by the second order effect of the Hessian bound in our computations, which mostly affects the radius of large balls and not so much the radius of smaller balls, the latter being more critical to the size of the estimated ROA.

B. Three-dimensional system

We consider the Lorenz system in the regime where it admits a stable origin:

$$\begin{aligned} \dot{x}_1 &= 10\,(x_2 - x_1) \\ \dot{x}_2 &= x_1\,(0.5 - x_3) - x_2 \\ \dot{x}_3 &= x_1\,x_2 - \frac{8}{3}x_3. \end{aligned}$$

Data points are distributed over a uniform $50 \times 50 \times 50$ grid in $[-3, 3]^3$, and generated with the sampling time $\Delta t = 1.5$. The Hessian bound is equal to $\overline{H} = 1.19$ (estimated numerically). A good approximation of the ROA is obtained (Figure 2(b)), but the attractive set is quite large (Figure 2(a)). This could be improved with a larger number of data points around the equilibrium. However, the method is computationally expensive in this three-dimensional case, mostly due to the possibly large number of required data points and the use of an adaptive grid. It should therefore be adapted to tackle higher-dimensional systems (see Section V).

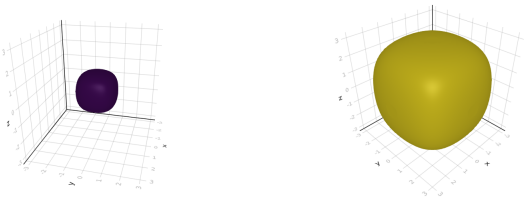

(a) Attractive set (b) Approximation of the ROA

Fig. 2. For the Lorenz dynamics, the method shows that Ω_{α_1} (blue set in (a)) is attractive in the inner approximation Ω_{α_0} (yellow set in (b)) of the ROA. Both subfigures are on the same scale

V. Conclusion

We have developed a novel method for ROA estimation in a purely data-driven setting, where both construction and validation of a Lyapunov function are performed on a pre-defined dataset generated by an unknown flow map. The Lyapunov function is obtained through a data-driven approximation of the Koopman operator associated with the flow map, and the validation step relies on the computation of bounds on the gradient of the Lyapunov function and the estimation of local Lipschitz constants of the flow map from the data. This method provides formal stability certificates with the sole knowledge of a (possibly loose) bound on the norm of the Hessian matrix of the flow map.

We envision several perspectives for future research. Since the validation step relies on a branch-and-bound method based on an adaptive grid, it does not scale well with system dimension and cannot be used with high-dimensional systems. For these cases, the validation step could be performed through the probabilistic scenario approach [3]. The use of other basis functions (possibly well-suited to high dimensions, such as radial basis functions) could be investigated, but would require to adapt the validation step. Moreover, the shape of sublevel sets of Lyapunov functions does not properly adapts to the geometry of the ROA. This could be improved by considering an additional optimization step on the weight matrix $\mathbf{\Sigma}$. Finally, the method could be extended to systems with outputs and used to compute controlled invariant sets.

VI. Acknowledgments

A. Mauroy thanks Peter Benner for suggesting the idea of computing local Lipschitz constants from data. Numerical experiments have been performed in Julia, with additional Julia packages: *LinearAlgebra, Statistics, ControlSystems, DifferentialEquations [11], MatrixEquations, LazyGrids, NearestNeighbors*. This research used resources of the "Plateforme Technologique de Calcul Intensif (PTCI)" located at the University of Namur, Belgium, which is supported by the FNRS-FRFC, the Walloon Region, and the University of Namur (Conventions No. 2.5020.11, GEQ U.G006.15, 1610468, RW/GEQ2016 et U.G011.22). The PTCI is member of the "Consortium des Equipements de Calcul Intensif (CECI)".

References

[1] B. Bánhelyi, E. Palatinus, and B. L. Lévai. Optimal circle covering problems and their applications. *Central European Journal of Operations Research*, 23(4):815–832, 2015.

[2] R. Bobiti and M. Lazar. A sampling approach to finding Lyapunov functions for nonlinear discrete-time systems. In *2016 European Control Conference (ECC)*, pages 561–566. IEEE, 2016.

[3] G. C. Calafiore and M. C. Campi. The scenario approach to robust control design. *IEEE Transactions on automatic control*, 51(5):742–753, 2006.

[4] H.-D. Chiang, M. W. Hirsch, and F. F. Wu. Stability regions of nonlinear autonomous dynamical systems. *IEEE Transactions on Automatic Control*, 33(1):16–27, 1988.

[5] S. A. Deka, A. M. Valle, and C. J. Tomlin. Koopman-based neural Lyapunov functions for general attractors. In *2022 IEEE 61st Conference on Decision and Control (CDC)*, pages 5123–5128. IEEE, 2022.

[6] J. Kenanian, A. Balkan, R. M. Jungers, and P. Tabuada. Data driven stability analysis of black-box switched linear systems. *Automatica*, 109:108533, 2019.

[7] M. Korda. Computing controlled invariant sets from data using convex optimization. *SIAM Journal on Control and Optimization*, 58(5):2871–2899, 2020.

[8] A. Mauroy and I. Mezić. Global stability analysis using the eigenfunctions of the Koopman operator. *IEEE Tran Autom Control*, 61(11):3356–3369, 2016.

[9] A. Mauroy, A. Sootla, and I. Mezić. Koopman Framework for Global Stability Analysis. In A. Mauroy, Y. Susuki, and I. Mezić, editors, *Koopman operator in systems and control*, pages 35–58. Springer, 2020.

[10] A. Mauroy, Y. Susuki, and I. Mezić. *Koopman operator in systems and control*. Springer, 2020.

[11] C. Rackauckas and Q. Nie. Differentialequations.jl–a performant and feature-rich ecosystem for solving differential equations in julia. *Journal of Open Research Software*, 5(1), 2017.

[12] S. M. Richards, F. Berkenkamp, and A. Krause. The Lyapunov neural network: Adaptive stability certification for safe learning of dynamical systems. In *Conference on Robot Learning*, pages 466–476. PMLR, 2018.

[13] U. Topcu, A. K. Packard, P. Seiler, and G. J. Balas. Robust region-of-attraction estimation. *IEEE Transactions on Automatic Control*, 55(1):137–142, 2009.

[14] G. Valmorbida and J. Anderson. Region of attraction estimation using invariant sets and rational Lyapunov functions. *Automatica*, 75:37–45, 2017.

[15] M. O. Williams, I. G. Kevrekidis, and C. W. Rowley. A data–driven approximation of the Koopman operator: Extending dynamic mode decomposition. *Journal of Nonlinear Science*, 25(6):1307–1346, 2015.

[16] L. Zheng, X. Liu, Y. Xu, W. Hu, and C. Liu. Data-driven estimation for region of attraction for transient stability using Koopman operator. *CSEE Journal of Power and Energy Systems*, 2022.

[17] K. Zhou, J. C. Doyle, and K. Glover. *Robust and optimal control*. Prentice Hall New Jersey, 1996.

Appendix

A. Computation of the matrices $\mathbf{W}$ and $\mathbf{Z}$ in (5)

We need to find the weighting matrices satisfying

$$\mathbf{Q} - \mathbf{U}\mathbf{Q}\mathbf{U}^{\mathrm{T}} - \mathbf{W} - \mathbf{U}\mathbf{Q}(\mathbf{Z}-\mathbf{Q})^{-1}\mathbf{Q}\mathbf{U}^{\mathrm{T}} \succ \mathbf{0}.$$

Let us set $\mathbf{Z} = (\delta_Z^{-1}+1)\mathbf{Q}$, $\mathbf{W} = \delta_W\mathbf{Q}$ and then choose positive δ_Z, δ_W small enough to satisfy the constraints above. We have

$$\begin{aligned}\mathbf{0} &\prec \mathbf{Q} - \mathbf{U}\mathbf{Q}\mathbf{U} - \mathbf{W} - \mathbf{U}\mathbf{Q}(\mathbf{Z}-\mathbf{Q})^{-1}\mathbf{Q}\mathbf{U}^{\mathrm{T}} \\ &= \mathbf{S}^*\Sigma\mathbf{S} - \mathbf{S}^*\Lambda^*\Sigma\Lambda\mathbf{S} - \delta_W\mathbf{S}^*\Sigma\mathbf{S} - \delta_z\mathbf{S}^*\Lambda^*\Sigma\Lambda\mathbf{S}.\end{aligned}$$

This leads to the inequality $(1-\delta_W)\Sigma \succeq \Lambda^*\Sigma\Lambda(1+\delta_Z)$ and, since all the matrices are diagonal and Σ is positive definite, we have $\max_i |\lambda_i|^2 < (1-\delta_W)/(\delta_Z+1)$. On the other hand, if we use the condition

$$\begin{aligned}1 &\geq \|\mathbf{W}^{1/2}(\mathbf{I}z - \mathbf{L}^{\mathrm{T}})^{-1}\mathbf{Z}^{-1/2}\|_{\mathcal{H}_\infty} \\ &= \max_\omega \overline{\lambda}\left(\delta_W\Sigma(\mathbf{I}e^{j\omega}-\Lambda)^{-1}\frac{\delta_Z}{1+\delta_Z}\Sigma^{-1}(\mathbf{I}e^{j\omega}-\Lambda)^{-*}\right) \\ &= \frac{\delta_Z\delta_W}{1+\delta_Z}\left|1-\max_i|\lambda_i|\right|^{-2}\end{aligned}$$

we get the bound $\max_i|\lambda_i| \leq 1-\sqrt{\delta_Z\delta_W/(1+\delta_Z)}$. Since we have chosen a specific matrix $\mathbf{Q}$, our bounds relate according to $(1-\delta_W)/(\delta_Z+1) \leq \left(1-\sqrt{\delta_Z\delta_W/(1+\delta_Z)}\right)^2$, which is equivalent to $0 \leq ((1+\delta_Z)\delta_W - \delta_Z)^2$. Furthermore, the equality is achieved when $\delta_W = \delta_Z/(1+\delta_Z)$ and, in this case, we have $\max_i|\lambda_i| \leq 1-\delta_W$. It follows that we have finally $\mathbf{W} = \delta_W\mathbf{Q}$, $\mathbf{Z} = (\delta_Z^{-1}+1)\mathbf{Q} = \delta_W^{-1}\mathbf{Q}$ and we obtain (5) with $\delta = \delta_W$.

B. Computation of the bounds V_{max} and V_{min}

a) Computation of V_{max}: It follows from the triangular inequality that

$$\max_{\mathbf{x}\in\mathcal{R}(\mathbf{y}_k,r)} V(\mathbf{x}) \leq \sum_{i,j}\max_{\mathbf{x}\in\mathcal{R}(\mathbf{y}_k,r)}(\mathbf{Q}_{ij}\psi_i(\mathbf{x})\psi_j(\mathbf{x})) \triangleq V_{max}\,. \tag{11}$$

In the case of monotone functions ψ_i (e.g. monomials), the maximal value of each term is attained at the vertices of $\mathcal{R}(\mathbf{y}_k,r)$ (except if $|y_k^{(l)}| \leq r_k\,L_l(\mathbf{x}_k) + \overline{H}\,r_k^2$ for some $l=1,\dots,n$, in which case 0 could be the maximal value).

b) Computation of V_{min}: The minimal value of V over the ball $\mathcal{B}(\mathbf{x}_k,r)$ lies on the boundary $\partial\mathcal{B}(\mathbf{x}_k,r)$, provided that the function V has no stationary point inside the ball (only the origin in the case of monomial basis functions). It follows that one can compute the values of V at uniformly distributed sample points $\mathbf{z}_j \in \partial\mathcal{B}(\mathbf{x}_k,r)$ and get

$$\min_{\mathbf{x}\in\mathcal{B}(\mathbf{x}_k,r)} V(\mathbf{x}) \geq \min_j \mathbf{z}_j - h\max_{\mathbf{x}\in\mathcal{B}(\mathbf{x}_k,r)}\|\nabla V(\mathbf{x})\|$$

with the filling distance $h = \max_{\mathbf{x}\in\partial\mathcal{B}(\mathbf{x}_k,r)}\min_j\|\mathbf{x}-\mathbf{z}_j\|$. The second term is a margin that takes into account the inaccuracy due to the sampling. The maximal value of the norm $\|\nabla V(\mathbf{x})\|$ over $\mathcal{B}(\mathbf{x}_k,r)$ is obtained with (11) by considering a hyperrectangle $\mathbf{x}_k + [-r,r]^n \supset \mathcal{B}(\mathbf{x}_k,r)$ and noting that $\|\nabla V(\mathbf{x})\| = \tilde{\mathbf{\Psi}}^T\tilde{\mathbf{Q}}\tilde{\mathbf{\Psi}}$ where $\tilde{\mathbf{\Psi}}$ is a vector of monomials of the form $\frac{\partial\psi_i}{\partial x_l}\psi_j$ and $\tilde{\mathbf{Q}} \succ \mathbf{0}$.